Preprints of the 19th World Congress
The International Federation of Automatic Control
Cape Town, South Africa. August 24-29, 2014

MIMO H_∞ control for power source coordination – application to energy management systems of electric vehicles

W. Nwesaty, A. I. Bratcu, O. Sename

Grenoble Institute of Technology, GIPSA-lab, Control Systems Department, 38402, Saint-Martin d'Heres, France. e-mail: (waleed.nwesaty, antoneta.bratcu, olivier.sename) @gipsa-lab.grenoble-inp.fr

Abstract: This paper deals with a control strategy used for designing energy management systems within average-power electric vehicles. The power supply system is composed of three sources, namely a fuel cell, a battery and an ultracapacitor – specialized within distinct frequency ranges – which must be coordinated in order to satisfy power demand of the vehicle's electrical motor. The three sources with their associated DC-DC converters are paralleled on a common DC-bus supplying the electrical motor. The DC-bus is required to be constant regardless of the load state thanks to the fuel cell which provides the mean power and to the other two sources – auxiliary sources – which are controlled to supply the high-frequency variations of power demand according to an H_∞ optimization strategy. MATLAB®/Simulink® numerical simulation is used to validate the proposed strategy under real driving cycle condition proposed by IFSTTAR (Institut Français des Sciences et Technologies des Transports, de l'Aménagement et des Réseaux), and this approach is assessed against another optimal strategy that uses LQR as control design.

Keywords: H_∞ control, Optimal power flow, Electric vehicles, Energy management systems, Multi sources power supply system.

1. INTRODUCTION

Electric vehicles are the key to solve problems concerning pollution issue due to their zero CO_2 and noise emission; moreover, they are relatively cheap compared to the growing petrol prices (Florescu et al., 2012a). Many research works are performed in this field to find clean power sources as fuel cells or photovoltaic panels, and also to develop on-board energy management systems in order to maximize efficiency of energy consumption (Li and Liu, 2009). Alternately, auxiliary power sources – like batteries and ultracapacitors – are used not only to energize the different electrical peripherals in the vehicle, but also to collect kinetic energy whenever the vehicle slows down or stops which also leads to maximize the efficiency of the power system. On the other hand, several studies have reported that the use of the fuel cell for automotive applications is limited by the slow transient and the oxygen starvation phenomena. In addition, the large current ripple allowed to the fuel cell and the battery may shorten their lifetime (Ozatay et al. (2004); Iannuzzi (2007)). All these constraints make it more challenging to design an efficient energy-management system and a power-sharing method involving fuel cells, batteries and ultracapacitors. There are two terms to describe a power source with respect to its power supply ability (Thounthong et al., 2009) as described here after:

- source with high energy density which is able to provide power during a long period of time with slow dynamic characteristics; fuel cells and batteries belong to this class of sources, and
- source with high power density which is able to provide high power for a short period of time with high dynamic characteristics; ultracapacitors are typical examples of such type of sources.

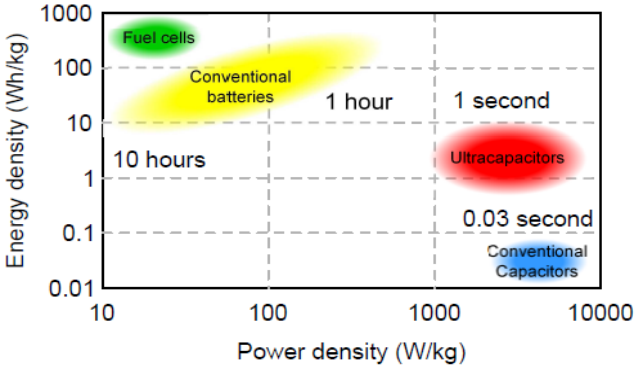

Fig. 1. Characteristics of different power sources (Ragone's plot): fuel cells as high-energy-density sources and ultracapacitor as high-power-density sources at extremes.

This classification is shown by Ragone's chart (Fig. 1) (Kuperman and Aharon, 2011). According to it, ultracapacitors have high power density since they can provide several kilowatts in less than a second. This property makes ultracapacitors correspond to abruptly varying loads. On

the contrary, fuel cells can provide power for several hours when load is in steady state or for charging other auxiliary sources like battery and ultracapacitor. Thus, fuel cells are well suited to provide energy when power demand varies very slowly.

This paper deals with power flow coordination between three power sources – fuel cell, battery and ultracapacitor – within an electrical vehicle, each one of the sources is controlled by means of a DC-DC converter. Sources are connected in parallel to the load (consisting of an electrical motor with its associated converter) through a DC-bus (Fig. 2). The fuel cell is considered as the main source of power and connected to a 1-quadrant boost converter which only allows unidirectional power flow, whereas the battery and the ultracapacitor represent auxiliary sources able to cover variations of power demand that are placed in relatively high frequency. In this way, the lifetime of the main source is extended by restricting its utilization at low frequency. Each auxiliary source is connected to a 2-quadrant boost converter which allows charging/discharging. The full electrical schematic of the system is shown in Fig. 2. The element values are provided in the Appendix A.

The control objective is to regulate the DC-bus voltage at 150 V with a tracking error of ±10 V in the presence of load power perturbation. This is achieved thanks to power flow coordination between sources with respect to their frequency characteristics, which in consequence leads to improve utilization and extend life of both fuel cell and battery.

In the literature, most of the studied systems consist of two power sources such as a fuel cell as main source and an auxiliary source like a battery or an ultracapacitor (Yu et al., 2011). In general, each source is treated as a current source whose current should be controlled according to a reference. The current reference is generated using different methods such as PID-controller-based strategies (Wong et al., 2011), fuzzy logic control (Fadel and Zhou, 2011), or strategies based on high/low-pass filtering of the global current reference in order to achieve frequency separation between the power sources (Florescu et al. (2012b); Florescu et al. (2012c)). LQG control can also be used to generate the current references (Florescu et al., 2012a).

This paper proposes an application of H_∞ control to coordinate efficiently auxiliary power sources –battery and ultracapacitor–. The same problem has recently been approached by means of Linear Parameter Varying (LPV) control (Nwesaty et al., 2014). Different from this paper, given that the global system exhibits bilinear dynamics, current references are here generated by H_∞ control synthesis which guarantees the global stability of the closed-loop system and specifies the frequency domain use of each source by means of the associated weighting functions. The current references generated by this algorithm cover the high-frequency variations of load current, while the fuel cell is supposed to supply the steady-state load current –mean value–. A PI controller is used to generate the required fuel cell's current reference by regulating the DC-bus voltage within a cascade control structure. Note that each auxiliary source's current reference is generated in two stages, as follows: one stage is used to regulate the

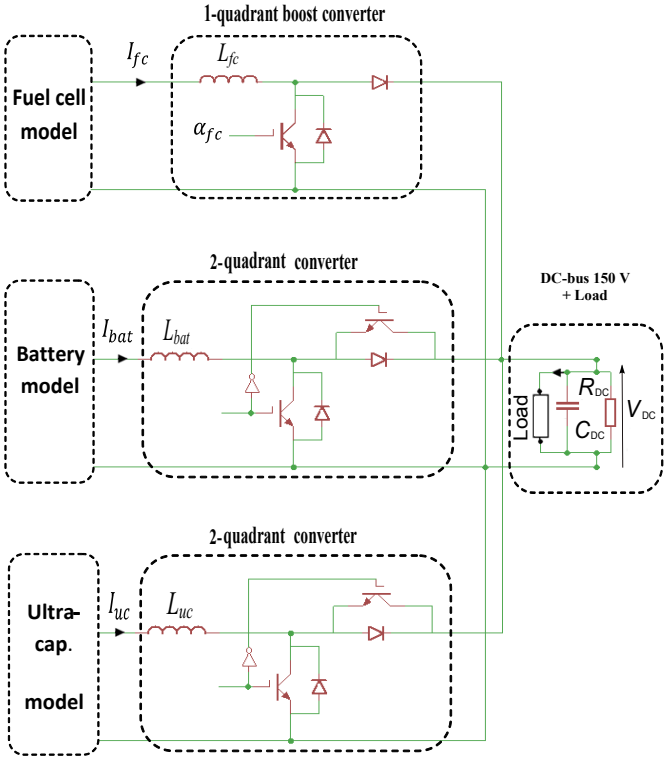

Fig. 2. System block and electrical representation.

state of charge (SOC) with a slow dynamic, thus providing the low-frequency component of current reference to the low-level current control loop –which has fast dynamic–. The other stage provides the high-frequency component of current reference, which is computed according to the proposed H_∞ control strategy (Fig. 3).

2. MODELING

The considered system consists of three power sources connected in parallel *via* DC-DC boost converters and finally attached to a single DC-bus which supplies power to the vehicle motor. The full electrical scheme of the system is represented in Fig. 2. The DC-bus voltage is supposed to be regulated by using a PI controller which generates the current reference of the main source –fuel cell–, whereas the auxiliary sources handle variations in power demand caused by the motor by using an H_∞ controller. The DC-DC converters are represented by their respective averaged models. Energy conservation laws lead to a nonlinear model and they are expressed by the following dynamic equations:

$$\dot{I}_{fc} = \frac{1}{L_{fc}}[V_{fc} - V_{dc}(1-\alpha_{fc})] \quad (1)$$

$$\dot{I}_{uc} = \frac{1}{L_{uc}}[V_{uc} - V_{dc}\alpha_{uc}] \quad (2)$$

$$\dot{I}_{bat} = \frac{1}{L_{bat}}[V_{bat} - V_{dc}\alpha_{bat}] \quad (3)$$

$$\dot{V}_{dc} = \frac{1}{C_{DC}}[\frac{-1}{R_{DC}}V_{dc} - I_{Load} + I_{fc}(1-\alpha_{fc}) + I_{bat}\alpha_{bat} + I_{uc}\alpha_{uc}] \quad (4)$$

$$I^*_{fc} = K_p e + K_i \int e \quad (5)$$

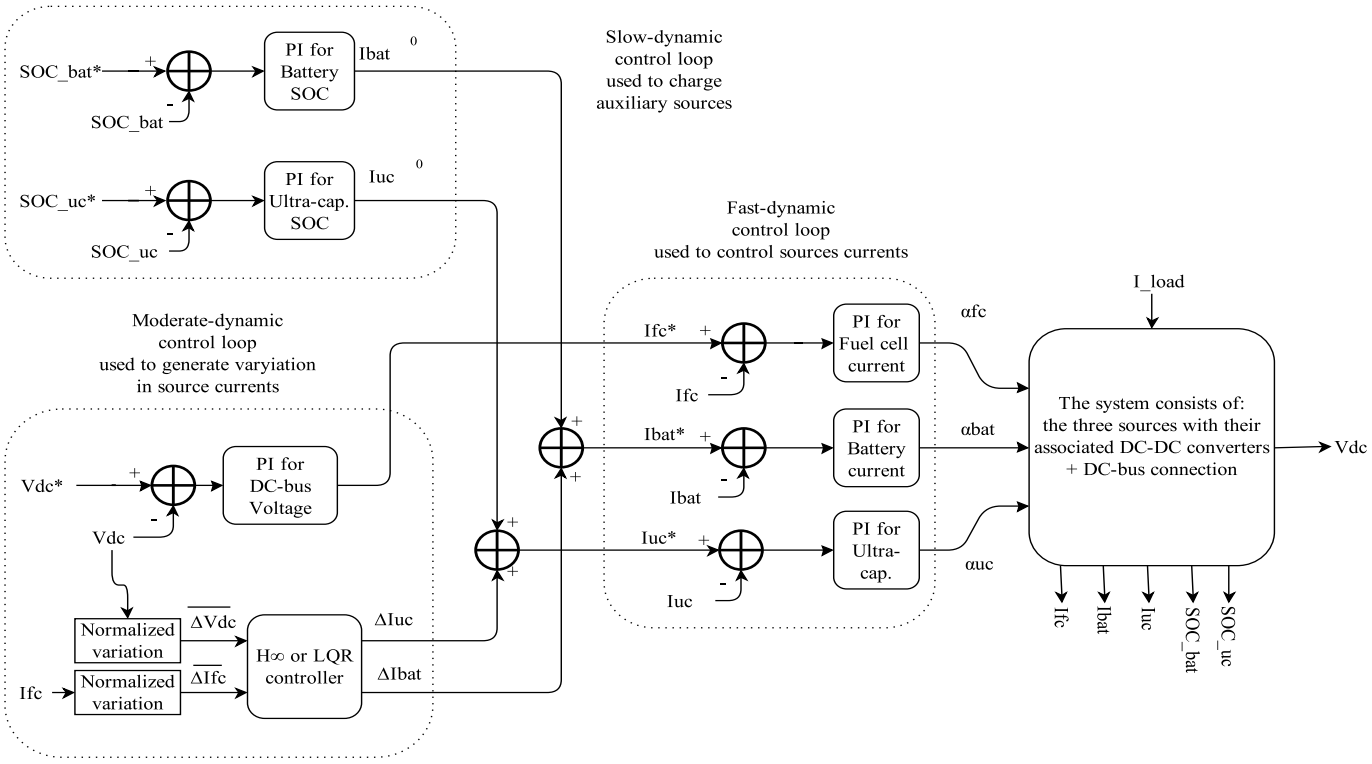

Fig. 3. Global control block diagram.

where I_{fc}, I_{bat}, and I_{uc} are currents of fuel cell, battery, and ultracapacitor, respectively. V_{fc}, V_{bat}, and V_{uc} are the respective source voltages. $\alpha_{fc}, \alpha_{bat}$, and α_{uc} are the respective converter duty ratios. C_{DC} and R_{DC} are the DC-bus capacitor and resistance, respectively. V_{dc} is the DC-bus voltage, I_{Load} is the load current. e is the DC-bus voltage tracking error. ${I_{fc}}^*$ is the fuel cell current reference. K_p and K_i are controller proportional and integral gain, respectively.

Equations (4) and (5) correspond to the DC-bus voltage closed-loop second-order dynamics. We are interested in its linearized model around different operating points defined by the DC-bus voltage setpoint, ${V_{dc}}^*$=150 V, and the different mean values of fuel cell current which corresponds to mean load current. By computing the normalized variations of the variables in (4) and (5) we obtain:

$$\left.\begin{aligned} \dot{\overline{\Delta V}}_{dc} &= \frac{1}{C_{DC}.V_{dc}^*}[\frac{-V_{dc}^*}{R_{DC}}.\overline{\Delta V}_{dc} \\ &\quad + (1-\alpha_{fc}).I_{fc}^*.\overline{\Delta I}_{fc} - \Delta I_{Load} \\ &\quad + \alpha_{bat}.\Delta I_{bat} + \alpha_{uc}.\Delta I_{uc}] \\ \dot{\overline{\Delta I}}_{fc} &= K_i.V_{dc}^*.\overline{\Delta V}_{dc} - K_p.\dot{\overline{\Delta V}}_{dc} \end{aligned}\right\} \quad (6)$$

where notation $\overline{\Delta x} = \frac{x-\widetilde{x}}{\widetilde{x}}$ denotes normalized variation in the desired operating point. $\widetilde{x}$ is the average value of x.The load current I_{Load} acts as a disturbance on system (6). The basic idea of the proposed control strategy is to consider variations of currents of the two auxiliary sources, ΔI_{bat} and ΔI_{uc}, as control inputs for system (6), which should result from requiring that disturbance to be rejected, as Fig. 3 shows. In this paper, ΔI_{bat} and ΔI_{uc} are generated by optimal control design, where controllers in each operating point of the working load interval comply with the requirement of separating sources in frequency. Thus, these controllers result from an H_∞ control design.

In the sequel, we will consider $I_{fc}^* = I_{fc}$ because the fuel cell current control loop exhibits a dynamic faster than that of the PI-controller-based loop generating I_{fc}^*(see Fig. 3).

3. CONTROL DESIGN

This section details the control approach used to coordinate the on-board power sources. The control objective is to handle the variation of power demand by the auxiliary sources, meanwhile ensuring the DC-bus voltage regulation at 150 V within an accepted error of $\pm 10V$. For this purpose an H_∞ controller is synthesized to guarantee frequency separation between the auxiliary sources (battery and ultracapacitor) and to keep the main source (fuel cell) supplying the mean power to the load. Fig. 3 shows the global control diagram of the system. All current control loops have fast closed-loop dynamics compared to the other control loops; therefore, they are grouped together. Similarly, state of charge (SOC) control loops are characterized by slow closed-loop dynamics and then they are also grouped together. Design of these loops is not detailed in this work (Åström and Hägglund, 1995). Measured values of voltages and currents are used as feedback variables for control purpose and supposed to be available in real time.

3.1 Current control loops

Current of each source must be controlled and prevented from exceeding admissible limits. To this end, PI-controller-based control loops are built around plant

transfer functions given by (1), (2) and (3), respectively. References of these control loops are provided by the outer loops, *i.e.*, by the DC-bus voltage loop for fuel cell current, by the battery SOC loop for battery current, by ultracapacitor SOC loop for ultracapacitor current and by the H_∞ control loop which generates the variation of the auxiliary sources' currents (see block control diagram in Fig. 3). PI controllers are designed according to imposed performance in terms of bandwidth and damping.

3.2 DC-bus voltage control loop

The fuel cell as main source is in charge with regulation of DC-bus voltage at reference value V_{dc}^*=150 V. A PI controller is used to this end – tuned analogously with current PI controllers – while the auxiliary sources (battery and ultracapacitor) are required to contribute for reducing variations of DC-bus voltage and fuel cell current.

3.3 State of charge control loops

States of charge of auxiliary sources are maintained within imposed limits – 0% and 100% of full charge – by generating the averaged components of the corresponding current references, I_{bat}^0 and I_{uc}^0 (Fig. 3). Two PI controllers ensure that battery and ultracapacitor be ready to use. Dynamics of these loops must be imposed slower than that of DC-bus voltage loop. Battery SOC reference is set at 100% – representing full charge – while ultracapacitor SOC reference is chosen 50% to preserve source capability to absorb/provide high currents in response to load current variation.

3.4 H_∞ control design

Equation (6) shows the second-order dynamics corresponding to the DC-bus voltage closed-loop, this can also be represented as:

$$\begin{cases} \dot{x} = A \cdot x + B_1 \cdot \omega + B_2 \cdot u \\ y \quad\quad = [1 \quad 0]x \end{cases} \tag{7}$$

with matrices

$$A = \begin{bmatrix} \dfrac{-1}{C_{DC} \cdot R_{DC}} & \dfrac{(1-\alpha_{fc}) \cdot I_{fc}^*}{C_{DC} \cdot V_{dc}^*} \\ \left(\dfrac{K_p \cdot V_{dc}^*}{C_{DC} \cdot R_{DC} . I_{fc}^*} - \dfrac{K_i \cdot V_{dc}^*}{I_{fc}^*}\right) & -\dfrac{(1-\alpha_{fc}) \cdot K_p}{C_{DC}} \end{bmatrix}$$

$$B_1 = \begin{bmatrix} \dfrac{-1}{C_{DC} \cdot V_{dc}^*} \\ \dfrac{K_p}{C_{DC} \cdot I_{fc}^*} \end{bmatrix} \quad B_2 = \begin{bmatrix} \dfrac{\alpha_{bat}}{C_{DC} \cdot V_{dc}^*} & \dfrac{\alpha_{uc}}{C_{DC} \cdot V_{dc}^*} \\ -\dfrac{K_p \alpha_{bat}}{C_{DC} \cdot I_{fc}^*} & -\dfrac{K_p \alpha_{uc}}{C_{DC} \cdot I_{fc}^*} \end{bmatrix}$$

where state vector $x = [\overline{\Delta V}_{dc} \quad \overline{\Delta I}_{fc}]^T$ is composed of DC-bus voltage and fuel cell current normalized variations around the chosen operating point, respectively, $\omega = \Delta I_{Load}$ is load current variation, which represents the disturbance input, $u = [\Delta I_{bat} \quad \Delta I_{uc}]^T$ is the control input vector composed of variations of battery and ultracapacitor current, respectively. The objective is to minimize the variations of DC-bus voltage and also the variations of the fuel cell current by varying battery and ultracapacitor currents in the desired frequency ranges. The control formulation is considered in the H_∞ framework as represented in Fig. 4. The generalized plant has three inputs, namely, the load –electrical motor– current, which is considered as disturbance input, and variations of auxiliary sources' currents, which are the control inputs. Plant outputs are the DC-bus voltage variation, which should be minimized to be within $\pm 10V$ around setpoint, and the variation of the fuel cell current. The selection of weighting functions is the key to confine the contribution of each source within a desired frequency range. The DC-bus voltage tracking error is bounded by using a first-order weighting function($W_{e\Delta V_{dc}}$). Fuel cell is kept supplying power in the low-frequency range, and the variation of its current is bounded by a first-order weighting function ($W_{e\Delta I_{fc}}$) as well. The battery and ultracapacitor roles are bounded by a low-pass, $W_{u\Delta I_{bat}}$, and a band-pass weighting function, $W_{u\Delta I_{uc}}$, respectively, that correspond to fourth-order filters, as shown in Fig. 5. These relatively high-order filters have been chosen to ensure more distinct frequency separation. The bandwidth of each source is chosen as $\omega_{n\Delta I_{fc}}$=0.05 rad/s, $\omega_{n\Delta I_{bat}}$=0.1 rad/s and $\omega_{n\Delta I_{uc}}$=1 rad/s. according to the desired performance and source types (*e.g.*, maximum admissible current gradient).

Several operating points are taken into account to linearize the system; these points are determined by the fuel cell current averaged value I_{fc}^* and DC-bus voltage setpoint V_{dc}^*=150 V. An H_∞ controller $K_i = \begin{bmatrix} A_i & B_i \\ C_i & D_i \end{bmatrix}$ is synthesized for each operating point. Depending on the load current actual value, a first-order interpolation is made which involves its nearest two neighbor operating points. The optimization problem is represented by a set of linear matrix inequalities and solved using Yalmip/Sedumi solver (Poussot-Vassal (2008); Apkarian et al. (1995)). Existence of an unique Lyapunov function has also been verified, which guarantees overall closed-loop stability.

4. SIMULATION RESULTS

MATLAB®/Simulink® numerical simulation is performed to prove the effectiveness of the proposed power source coordination method. A comparison with an LQR– Linear Quadratic Regulator–control-based solution is provided. Nonlinear electrical models (1), (2), (3) and (4) are used for simulation purpose. A driving cycle with rich high-frequency content proposed by IFSTTAR (Institut Français des Sciences et Technologies des Transports, de l'Aménagement et des Réseaux) is used to apply variable power load demand (Fig. 6). This profile represents various driving conditions including acceleration, deceleration,

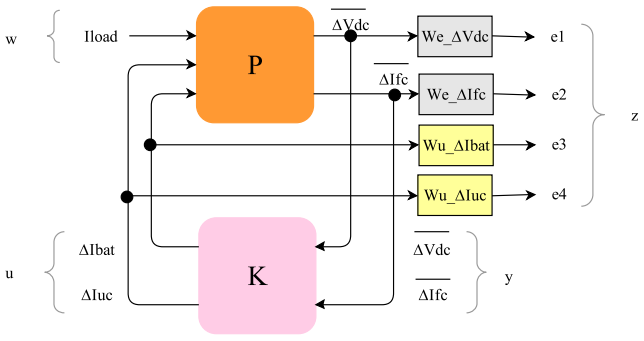

Fig. 4. H_∞ Robust control design block diagram.

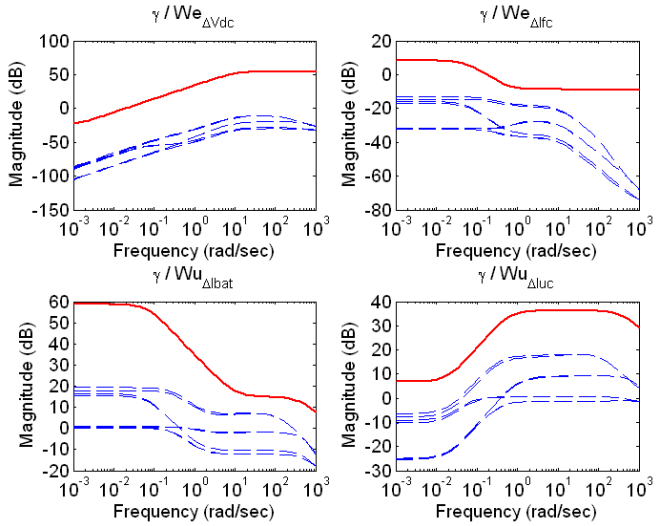

Fig. 5. Weighting function used to confine frequency ranges of battery and ultracapacitor current variations within imposed frequency domains.

steady speed and full brake and allows assessing performance of DC-bus voltage regulation and the way how the three sources are coordinated to provide the needed power.

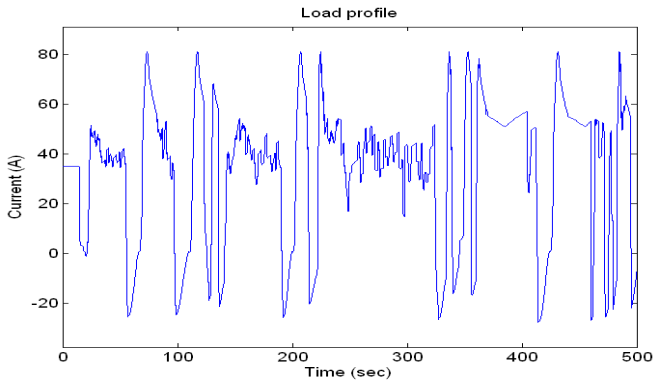

Fig. 6. IFSTTAR load current profile used in simulation.

4.1 LQR optimization method

We used another optimal control method, namely LQR for a comparative evaluation of performance of the H_∞ approach. Like the proposed approach, the LQR optimization method is used to synthesize a controller K_i at each operating point for the linearized system in (7), then, depending on the load current actual value, a first-order interpolation is made between its two neighbor operating points. This approach is also used to generate current references for the auxiliary power sources in the system, battery and ultracapacitor, according to the method proposed in (Florescu et al., 2012a), and aiming at minimizing the criterion $I = \lim_{T\to\infty} \frac{1}{T} \int_0^T [\Delta I_{fc}^2 + \beta I_{bat}^2 + \lambda I_{uc}^2]\mathrm{dt}$, where β and λ are the weighting factors that adjust the trade-off between fuel cell current variations and variations of auxiliary sources' currents. Fig. 7 shows that fuel cell current is smoothed while the DC-bus voltage is regulated to the reference value (150 V)(Fig. 8). The amplitude variation of battery current is reduced in detriment of ultracapacitor current variation. The drawback is that the two auxiliary sources cannot be separated in frequency domain; only amplitudes of their variations are different. To show that, further analysis of sources' currents is performed by computing the power spectral density (PSD) of each one. Since the amount of power delivered by each source is different, normalization of these densities is done with respect to the maximum power of each source in order to be comparable. The percentage of power supplied by each source and the corresponding frequency ranges are shown in Fig. 9. The H_∞ method adds flexibility to the control design because it allows frequency separation by means of appropriate choice of weighting functions.

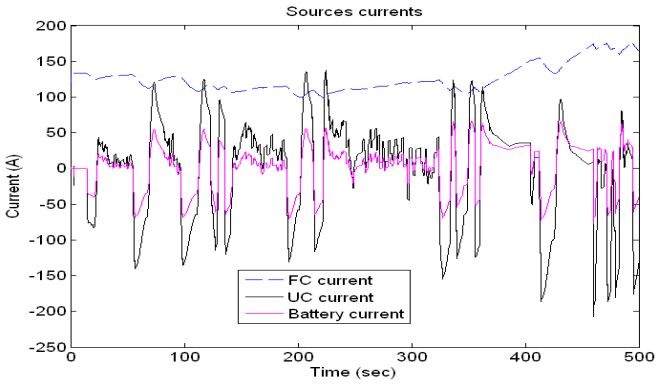

Fig. 7. Sources' currents according to LQR approach.

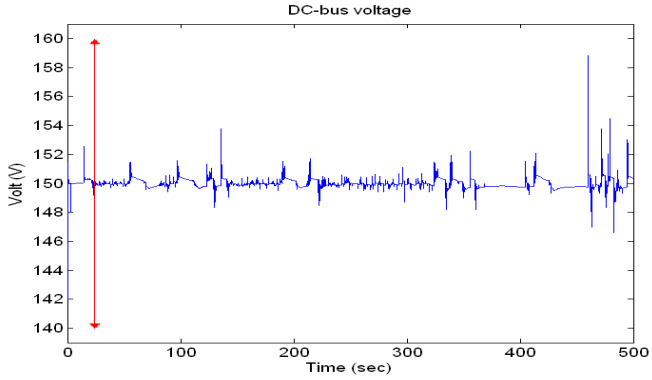

Fig. 8. DC-bus voltage well regulated around 150 $\pm 10V$ according to LQR approach.

4.2 H_∞ optimization method

One can see that the system is able to provide the demanded power and the DC-bus voltage shown in Fig. 10 is well regulated to reference 150 V within the allowed error $\pm 10V$. Fig. 11 shows how currents of different sources are provided to the system, with fuel cell supplying the average current and ultracapacitor handling the peak variations, while battery provides the midrange-frequency current. Normalized PSD also is calculated for each power source (Fig. 12). According to it, the frequency separation of the three sources corresponds to the chosen weighting functions.

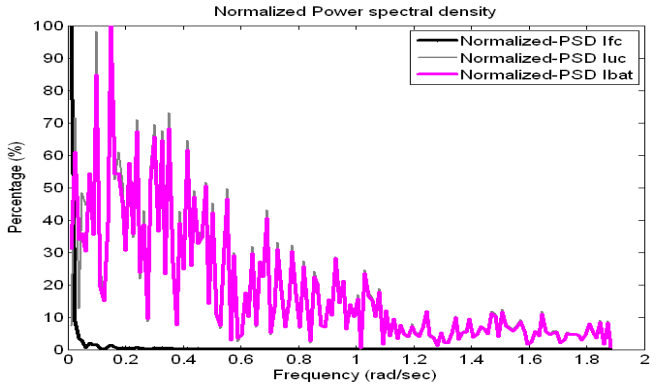

Fig. 9. Normalized power spectrum of the sources' currents corresponding to IFSTTAR load current profile by using LQR approach.

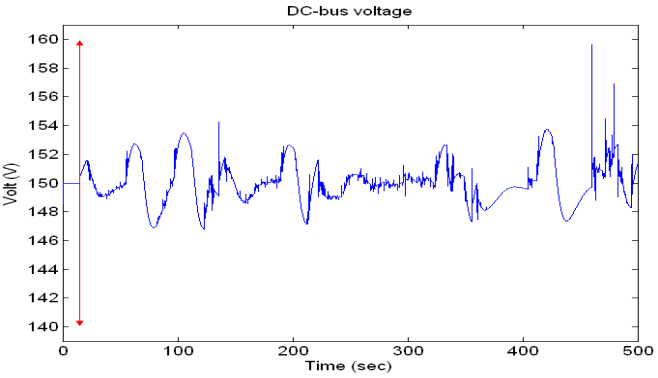

Fig. 10. DC-bus voltage well regulated around 150 $\pm 10V$ according to H_∞ approach.

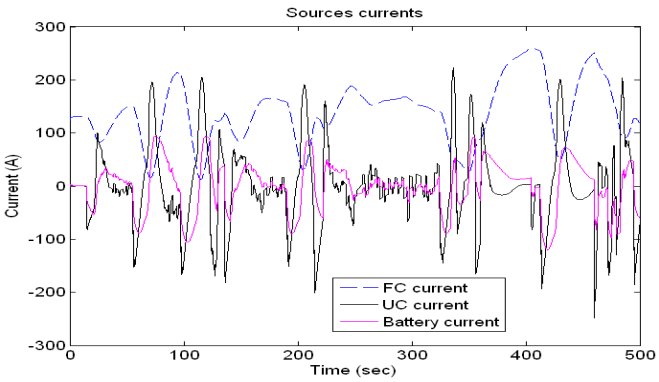

Fig. 11. Sources' currents according to H_∞ approach.

5. CONCLUSION

This paper has considered design of energy management strategy with guaranteed performance to be applied on board of an electric vehicle. This strategy is used to coordinate three different kinds of power sources represented by a fuel cell as main power source and two auxiliary sources, namely a battery and an ultracapacitor. This means that the fuel cell is managed to provide the mean power (low-frequency variations), whereas the battery and the ultracapacitor supply power in relatively high frequency. The ultracapacitor provides/absorbs the high-frequency content of load power in order to protect the other sources from sudden variation in power, and that helps to extend

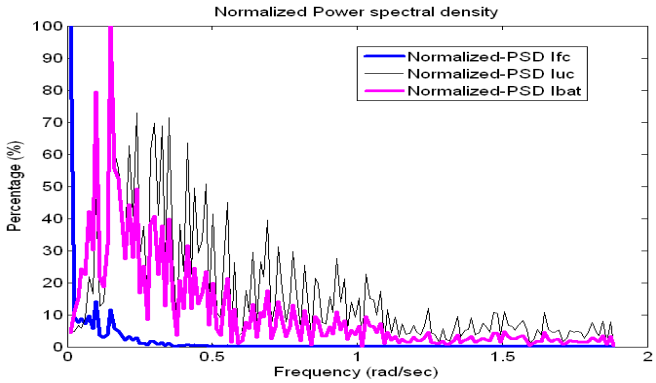

Fig. 12. Normalized power spectrum of the sources' currents corresponding to IFSTTAR load current profile by using H_∞ approach.

the life of both fuel cell and battery. The battery's role is placed in between the other two sources according to the frequency separation in the supplied load power, besides its role to energize the different peripherals within the vehicle.

Some test on representative driving cycle show that the proposed strategy is effective regarding the regulation of the DC-bus voltage and supplying the load power with respect to frequency separation between sources, in particular compared with an LQR optimal control which is not able to separate the frequency-domain use of auxiliary power sources' currents.

For future work, different power supply configurations can be analysed. For example, fuel cell could only be required to recharge the other sources at its maximum efficiency operating point, for sake of increasing the global power efficiency of the system. To this end, switching control could be applied to switch between two control laws taking into consideration two different system models, namely including/excluding the fuel cell.

Note also that the proposed power sharing strategy can easily be generalized to any kind of on-board energy management systems, potentially containing any number of power sources. Experimental validation should also be envisaged.

Appendix A.

Ultracapacitor converter: L_{uc}=0.5 mH; Battery converter: L_{bat}=0.5 mH; Fuel cell converter: L_{fc}=6 μH; DC-bus: V_{DC}=150 V, C_{DC}=22 mF, R_{DC}=100 kΩ. V_{dc} PI controller: $K_p = 71 \cdot 10^{-3}$,K_i =4.41.

REFERENCES

P. Apkarian, P. Gahinet, and G. Becker. Self-scheduled H_∞ control of linear parameter-varying systems: a design example. *Automatica*, 31(9):1251–1261, 1995.

A. Fadel and B. Zhou. An experimental and analytical comparison study of power management methodologies of fuel cell–battery hybrid vehicles. *Journal of Power Sources*, 196(6):3271 – 3279, 2011.

A. Florescu, A.I. Bratcu, I. Munteanu, and S. Bacha. Energy management system within electric vehicles using ultracapacitors: An LQG-optimal-control-based so-

lution. In *15th IFAC Workshop on Control Applications of Optimization*, Rimini, Italy, 2012a.

A. Florescu, I. Munteanu, A.I. Bratcu, and S. Bacha. Frequency-sepation-based energy management control strategy of power flows within electric vehicles using ultracapacitors. In *38th Annual Conference of the IEEE Industrial Electronics Society*, Montreal, Canada, 2012b.

A. Florescu, I. Munteanu, A.I. Bratcu, and S. Bacha. Results concerning ultracapacitor-based energy management strategy within electric vehicles. In *16th International Conference on System Theory, Control and Computing*, Sinaia, Romania, 2012c.

D. Iannuzzi. Use of supercapacitors, fuel cells and electrochemical batteries for electric road vehicles: A control strategy. In *The 33rd Annual Conference of the IEEE Industrial Electronics Society (IECON)*, pages 539–544, Taipei, Taiwan, NOV 5-8 2007.

A. Kuperman and I. Aharon. Battery–ultracapacitor hybrids for pulsed current loads: A review. *Renewable and Sustainable Energy Reviews*, 15(2):981 – 992, 2011.

C. Li and G. Liu. Optimal fuzzy power control and management of fuel cell/battery hybrid vehicles. *Journal of Power Sources*, 192(2):525 – 533, 2009.

W. Nwesaty, A.I. Bratcu, and O. Sename. LPV control for power source coordination – application to electric vehicles energy energy management systems. In 14^{th} *European Control Conference (ECC)*, Strasbourg, France, 2014. (Accepted for presentaion).

E. Ozatay, B. Zile, J. Anstrom, and S. Brennan. Power distribution control coordinating ultracapacitors and batteries for electric vehicles. In *American Control Conference*, pages 4716–4721, Boston Massachusetts,USA, 2004.

C. Poussot-Vassal. *Multi-variable LPV robust control for vehicle chasis (Commande Robuste LPV Multivariable de Chssis Automobile)*. PhD thesis, Grenoble INP, Grenoble, France, 2008.

K. J. Åström and T. Hägglund. *PID Controllers: Theory, Design, and Tuning*. Instrument Society of America, Research Triangle Park, NC, 2 edition, 1995.

P. Thounthong, S. Ral, and B. Davat. Energy management of fuel cell/battery/supercapacitor hybrid power source for vehicle applications. *Journal of Power Sources*, 193 (1):376 – 385, 2009.

J. H. Wong, N. R N Idris, M. Anwari, and T. Taufik. A parallel energy-sharing control for fuel cell-battery-ultracapacitor hybrid vehicle. In *Energy Conversion Congress and Exposition (ECCE), 2011 IEEE*, pages 2923–2929, 2011.

Z. Yu, D. Zinger, and A. Bose. An innovative optimal power allocation strategy for fuel cell, battery and supercapacitor hybrid electric vehicle. *Journal of Power Sources*, 196(4):2351 – 2359, 2011.